

Magnetic resonance imaging in children with sickle cell disease—detecting alterations in the apparent diffusion coefficient in hips with avascular necrosis

John D. MacKenzie · Andrea Hernandez ·
Andres Pena · Kai Ruppert · Dmitry Khrichenko ·
Leonardo Gonzalez · Abbas F. Jawad ·
Lawrence Wells · Kim Smith-Whitley · Diego Jaramillo

Received: 29 August 2011 / Revised: 5 December 2011 / Accepted: 8 December 2011 / Published online: 27 December 2011
© Springer-Verlag 2011

Abstract

Background Avascular necrosis (AVN) is a common morbidity in children with sickle cell disease (SCD) that leads to pain and joint immobility. However, the diagnosis is often uncertain or delayed.

J. D. MacKenzie · A. Hernandez · A. Pena · K. Ruppert ·
D. Khrichenko · L. Gonzalez · D. Jaramillo
Department of Pediatric Radiology,
Children's Hospital of Philadelphia,
Philadelphia, PA, USA

A. F. Jawad
Department of Pediatrics,
Children's Hospital of Philadelphia,
Philadelphia, PA, USA

L. Wells
Department of Orthopedics,
Children's Hospital of Philadelphia,
Philadelphia, PA, USA

K. Smith-Whitley
Department of Hematology,
Children's Hospital of Philadelphia,
Philadelphia, PA, USA

Present Address:

J. D. MacKenzie (✉)
Department of Radiology and Biomedical Imaging,
UCSF Benioff Children's Hospital,
505 Parnassus Ave,
San Francisco, CA 94143-0628, USA
e-mail: john.mackenzie@ucsf.edu

Present Address:

K. Ruppert
Department of Radiology,
University of Virginia,
Charlottesville, VA, USA

Objective To examine the ability of apparent diffusion coefficient (ADC) measurements on diffusion-weighted imaging to detect AVN in children with SCD.

Materials and methods ADC values were calculated at the hips of normal children ($n=19$) and children with SCD who were either asymptomatic with no known previous hip disease ($n=13$) or presented for the first time with clinical symptoms of hip pathology ($n=12$). ADC values were compared for differences among groups with and without AVN using non-parametric statistical methods.

Results The ADC values were elevated in the hips of children with AVN (median ADC= 1.57×10^{-3} mm²/s [95% confidence interval=0.86–2.10]) and differed significantly in pairwise comparisons (all $P<0.05$) from normal children (0.74 [0.46–0.98]), asymptomatic children with SCD (0.55 [0.25–0.85]), and SCD children who had symptoms referable to their hips but did not show findings of hip AVN on conventional MRI or radiographs (0.46 [0.18–0.72]).

Conclusion Children with sickle cell disease have elevated apparent diffusion coefficient values in their affected hips on initial diagnosis of avascular necrosis.

Keywords Sickle cell disease · Diffusion-weighted imaging · MRI · Avascular necrosis · Children

Introduction

Diffusion-weighted imaging (DWI) has been proposed as a complementary MR pulse sequence for pediatric musculoskeletal imaging [1]. Experimental data suggest that epiphyseal ischemia is detectable by DWI and that the information is complementary to, and more stable than the information

provided by perfusion imaging [2]. Hip ischemia in a piglet model of avascular necrosis (AVN) demonstrates initial restriction in diffusion with reduced blood flow. With increasing duration of ischemia, the diffusion increases rapidly and remains elevated [3–5] and in Legg-Calvé-Perthes disease, preliminary data indicate that epiphyseal diffusion varies with the stage of disease [5, 6].

The purpose of this study is to examine the potential for DWI with apparent diffusion coefficient (ADC) measurements to detect AVN in children with sickle cell disease (SCD). A noninvasive test that detects, and possibly may quantify AVN extent and severity AVN at an early stage, has the potential to aid in therapy decisions to slow the progression of hip joint dysfunction [7]. Children with SCD are at particular risk; approximately 50% will develop AVN by age 30 [8]. We hypothesize that altered water mobility resulting from the pathological processes of SCD (presumably vaso-occlusion and subsequent infarction) may be detected with ADC measurements.

Materials and methods

Population

Institutional review board (IRB) approval for this Health Insurance Portability and Accountability Act (HIPAA) compliant study was obtained, and the parent of each patient gave written informed consent. Forty-four children were enrolled prospectively for evaluation of their hips with DWI and the SCD children were enrolled consecutively over a 2-year period. All subjects were selected to be between the ages of 9 and 20 years. We selected 9 years as the lower bounds because this is the age when children with SCD begin to develop hip AVN. Age, sex, presence or absence and side of hip symptoms, clinical history and the ADC value were recorded for each child.

Children were placed into four groups (Table 1). The first group ($n=19$) consisted of children who had MRI for unrelated pathologies remote from the hips. These children were assumed to have normal hips on the basis of history and had no known bone marrow pathology: no history of AVN, no

systemic bone marrow disorder and no medication use that may alter bone marrow composition such as steroids or chemotherapy. Their hips were also screened with MRI for hip pathology (see below). These children in the normal group were referred for neuroimaging ($n=8$), musculoskeletal imaging of the extremities for problems remote from the hips ($n=9$), and ovarian masses prior to treatment ($n=2$). Indications for neuroimaging included headaches, diabetes insipidus, posterior fossa cyst, recurrent otitis media, resected craniopharyngioma off therapy, seizures, sensorineural hearing loss and back pain. Indications for musculoskeletal imaging of the extremities remote from the hips included shoulder pain with Bankart lesion, vascular malformation localized to the ankle, knee pain, lump on thigh remote from hips, recurrent patellar dislocation, elbow pain and wrist pain.

The second group consisted of children with SCD but without hip pain or evidence of AVN ($n=13$). The SCD children in this group were referred for MRI to address clinical questions unrelated to AVN or hip pathology and most subjects in this group were referred for brain MRI to screen for vaso-occlusive disease in the central nervous system. Eleven of these children had SS disease, one had SC and one had sickle beta-zero (β^0) thalassemia.

The absence of AVN and other hip pathology was confirmed in these two control groups by the lack of marrow edema on DWI and the normal anatomical appearance of the hips on coronal true fast imaging with steady-state precession (TrueFISP) obtained just prior to DWI. TrueFISP was selected to screen for hip pathology due to its rapid acquisition time of approximately 1 min, sensitivity to marrow pathology and ability to display architectural integrity of the hip without the need for radiography (Fig. 1). Although stage I AVN with bone marrow edema may be missed with this TrueFISP screening examination, the absence of marrow edema was confirmed on the subsequent T₂-weighted spin-echo echo-planar $b=0$ images.

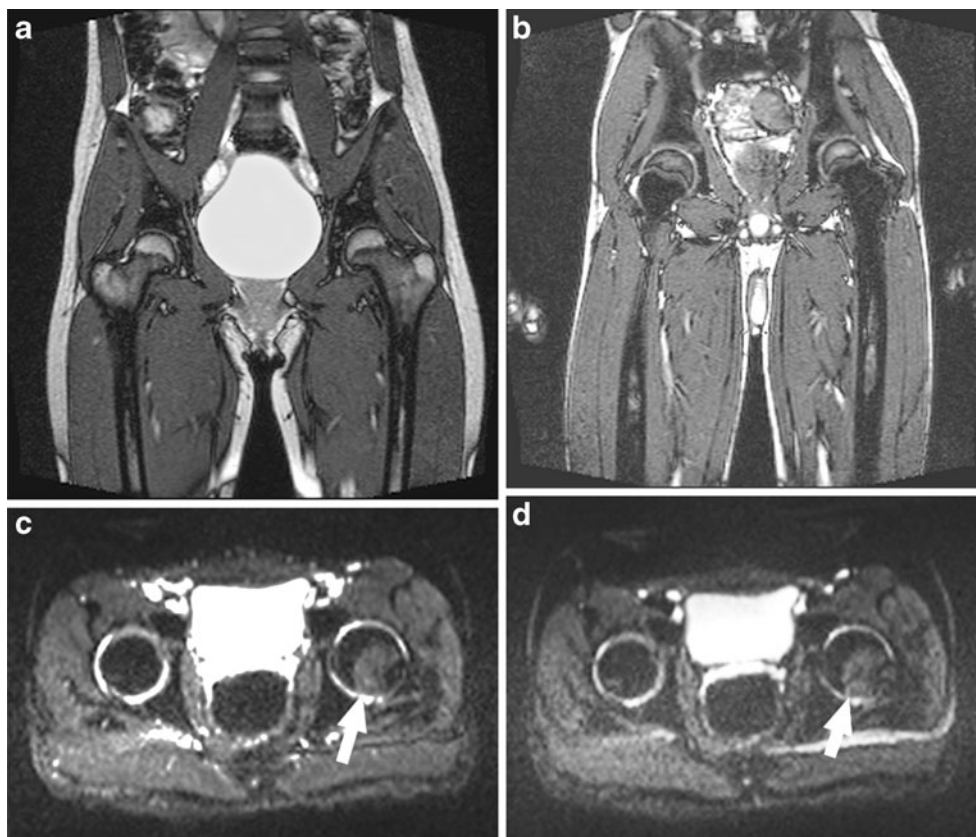
The third and fourth groups consisted of children with SCD who were imaged for possible new hip AVN ($n=12$). These children were referred to MRI for evaluation of suspected hip AVN based on history and clinical examination taken by a pediatric hematologist specializing in sickle cell disorders. Nine of these children had SS disease, two

Table 1 Demographics of children who were evaluated with diffusion-weighted imaging

	Normal children	Asymptomatic SCD without AVN	Symptomatic SCD without AVN	Symptomatic SCD with AVN
Male	9	9	2	5
Female	10	4	4	1
Age (mean±SD)	13.6±2.5	13.2±3.6	13.6±3.0	14.5±4.1
Age (median)	13.6	12.5	12.7	14.5
Age (range)	10.0–18.4	9.2–19.6	11.0–19.0	9.0–18.0

Data are numbers of patients (male and female), age in years. AVN avascular necrosis, SCD sickle cell disease

Fig. 1 Screening for avascular necrosis and other hip pathology with true fast imaging with steady state precession (TrueFisp). **a** Normal appearance of the hips in a 14-year-old girl on coronal TrueFISP (TR/TE, 4.14/2.07 ms; flip angle, 68°, slice thickness, 4 mm). **b–d** A 14-year-old boy with sickle cell disease (SCD) who did not have AVN: **b** TrueFisp shows structural integrity of the hips and replacement of the marrow fat from SCD. **c, d** Spin-echo echo-planar diffusion-weighted imaging may screen for the absence of bone marrow edema and shows normal hip morphology and intermediate to low signal intensity on the **(c)** T₂-weighted $b=0$ and **(d)** $b=500$ images. The physis is also well demonstrated on DWI as an oblique band of increased signal intensity that is readily discernible from AVN (*arrow* in **c** and **d**)



had SC and one had sickle β^0 thalassemia. Inclusion criteria for this symptomatic SCD group included no history of hip AVN and signs/symptoms of suspected vaso-occlusive crisis/AVN. This group was further subdivided based on whether AVN was detected on conventional STIR, T₁- and T₂-weighted MRI of the hips.

Imaging protocol

Diffusion-weighted images in the axial plane were acquired through both hips using a fat-suppressed diffusion-weighted spin-echo echo-planar sequence with either eight b-values ($n=35$; $b=0, 150, 250, 500, 600, 750, 900, 1,050$ s/mm²), four b-values ($n=7$; $b=0, 250, 500, 750$ s/mm²) or ten b-values ($n=2$; $b=0, 50, 100, 150, 200, 250, 300, 400, 500, 750$ s/mm²); repetition time (TR) msec/echo time (TE) msec, 3,400/85; number of signals acquired, 3; field of view, 24 cm; slice thickness, 4 mm with 1-mm gap; and parallel imaging (table and torso coils with parallel imaging factor of 2). Imaging was performed on a 1.5-T (Avanto; Siemens Medical Systems, Erlangen, Germany) or 3.0-T scanner (Trio; Siemens Medical Systems, Erlangen, Germany) running VB13 software. For each child, both hips were imaged simultaneously and we chose the axial plane to minimize the susceptibility artifacts on the echo-planar images that tend to be magnified in the pelvis when imaging in coronal and sagittal planes.

Although varying the field strength was not anticipated to produce significant alterations in ADC values beyond perhaps a small effect due to increased susceptibility-based background gradients at higher field strength [9], since the subjects were studied at both 1.5 and 3.0 T, a spherical water phantom was used to test for possible differences in ADC values obtained at these two field strengths. ADC values were measured in a spherical phantom with the same pulse sequence parameters as used in the subjects with DWI performed with eight b-values. Furthermore, to test for differences in ADC measurements that may arise due to differences in the number of b-values obtained, DWI was also performed in the water phantom with the DWI pulse sequence modified for either two b-values ($b=0$ and $b=500$) or eight b-values as described above.

In the normal patients and SCD children without known or suspected AVN, coronal T₂-weighted TrueFISP (TR/TE, 4.14/2.07 ms; flip angle, 68°, slice thickness, 4 mm) was obtained through the hips to exclude clinically occult hip pathology. TrueFISP imaging is an opposed-phase, primarily T₂*-weighted sequence that is moderately sensitive for marrow pathology but less likely to reveal bone marrow edema or small lesions in the hips when compared to routine T₁-, T₂-weighted and STIR imaging. We selected TrueFISP imaging because of its speed of acquisition and ability to define hip anatomy and exclude gross pathology in the children who were unlikely to have hip abnormalities due

to their clinical history and lack of symptoms. In addition, the likelihood of missing AVN in the subjects who did not have standard water selective STIR or T₂-weighted fat-saturated imaging is probably low because T₂-weighted spin-echo echo-planar $b=0$ images should show the presence of water; thus, absence of AVN was confirmed by the lack of increased signal intensity in the femoral head epiphyses on the T₂-weighted spin-echo echo-planar $b=0$ images.

For all SCD children with a clinical suspicion of AVN, conventional MRI pulse sequences and radiographs with AP and frog leg views of the hips were obtained in addition to DWI. The conventional MRI pulse sequences tailored to detect AVN consisted of coronal and axial T₁-weighted (TR/TE=500/20 ms), coronal and sagittal STIR (TR/TE/TI=4,400/54/170 ms), and axial fat-suppressed T₂-weighted images (TR/TE=4,000/80 ms). AVN was classified on the radiographs and conventional MRI using the University of Pennsylvania (Steinberg) staging system [10]. This system classifies AVN into stage 0 (preclinical with absence of imaging findings), stage I (only bone marrow edema on MRI or increased uptake on bone scan with normal radiographs), stage II (cystic and sclerotic changes in femoral head), stage III (subchondral collapse without flattening), stage IV (flattening of the femoral head), stage V (joint space narrowing or acetabular changes) and stage VI (advanced degenerative changes). Stages I–V are further subdivided on the amount of the femoral head affected: A=mild (<15% of the head affected), B=moderate (15–30%) and C=severe (>30%).

Image analysis

Signal intensity (SI) measurements were obtained by drawing a region of interest (ROI) about the femoral head epiphyses on the diffusion-weighted images. Only areas of bone marrow in the epiphysis were captured on the ROI; the ROI was drawn at least one axial image superior to the growth plate and at least 2–3 mm away from the articular cartilage and subchondral bone to avoid partial volume effects (Fig. 2). The physis could be readily observed as a band of increased signal intensity on the $b=0$ images. A dual fellowship trained musculoskeletal and pediatric radiologist with 4 years of postgraduate experience drew the ROIs.

The signal intensities in each ROI were measured with the aid of software written in Interactive Data Language v6.2 (IDL; ITT Visual Information Solutions, Boulder, CO). For quantitative analysis of tissue-specific diffusion properties, the ADC was calculated from the slope of the semilog plot of the SI as a function of the b factor from two diffusion-weighted images according to the equation: $ADC = [-\ln(SI_1/SI_0)] / (b_1 - b_0)$, where SI_1 and SI_2 are the mean SIs from identical ROIs drawn on the diffusion-weighted images at two b values ($b_0=0$ and $b_1=500$) [11].

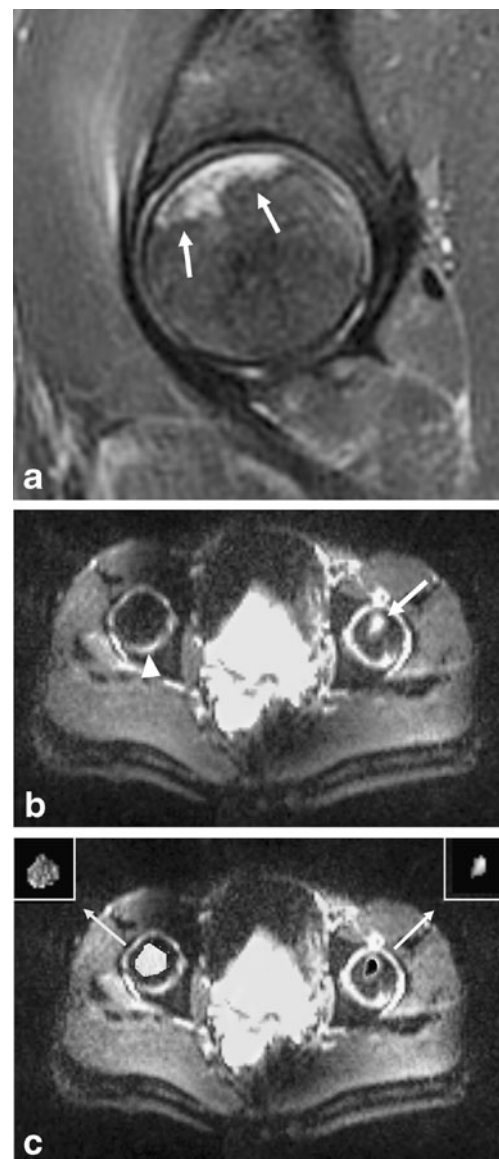


Fig. 2 Representative MR imaging of stage IA avascular necrosis (AVN) in a child with sickle cell disease. **a** Sagittal STIR image (TR/TE/TI=4,400/54/170 ms; slice thickness, 4 mm) shows AVN at the anterosuperior aspect of the right femoral head (arrows). **b** On the axial fat-suppressed T₂-weighted spin-echo echo-planar image (b -value, 0; TR/TE, 3,400/85; field of view, 24 cm; slice thickness, 4 mm), signal intensity is increased in the left femoral epiphysis with AVN (arrow). The increased signal intensity in the posterior aspect of the right proximal femur unaffected by AVN is from joint fluid (arrowhead) and is not included in the ROI analysis. **c** Region-of-interest analysis shows ADC values of $0.19 \times 10^{-3} \text{ mm}^2/\text{s}$ in the asymptomatic right hip and $2.10 \times 10^{-3} \text{ mm}^2/\text{s}$ in the left hip with AVN (arrows)

Data analysis

Agreement of ADC measurements between observers (the musculoskeletal/pediatric radiologist noted above and a medical student entering radiology residency) and between left and right hips was assessed by using the Bland-Altman method [12]. Median ADC values were tested for significant

differences among all groups with the Kruskal-Wallis test and for all pairs of groups using Dunn's post-test. Statistical calculations were performed using GraphPad Prism version 5.0 (GraphPad, San Diego, CA USA) and differences with a *P* value of less than 0.05 were considered significant.

Results

Measurement of ADC values showed acceptable agreement between readers and between the left and right control hips. The 95% limits of agreement for differences in ADC values ($\times 10^{-3}$ mm²/s) between observers was -0.35 to 0.30 with a bias of -0.03 and a standard deviation of the bias of 0.17 . Similarly, the 95% limits of agreement for differences in ADC values ($\times 10^{-3}$ mm²/s) between left and right hips in the normal children without hip pathology was -0.38 to 0.34 with a bias of -0.02 and a standard deviation of the bias of 0.18 .

Phantom data obtained at varying field strengths confirmed that no calibration would be needed for ADC measurements obtained in subjects between 1.5 and 3.0 T. Five separate ADC measurements obtained from a spherical water phantom were $1.97 \pm 0.00 \times 10^{-3}$ mm²/s at 1.5 T and 1.98 ± 0.01 at 3.0 T. Also, ADC values were not appreciably different when

obtained with only two b-values encoded into the pulse sequence (ADC = 1.96 ± 0.01 at 1.5 T).

The subject groups were not significantly different in their age or gender, *P* > 0.05 (Table 1). No children in both the normal group and the asymptomatic SCD group had MRI findings suggestive of AVN. For the 12 SCD children with hip symptoms, 6 showed no evidence of AVN in either femoral head on conventional STIR and T₁- and T₂-weighted MRI (Table 2). In four of these six, MRI demonstrated pathology that could explain their symptoms due to osteonecrosis outside the hip joint (e.g., in the iliac bone or femoral diaphysis, Table 2). The remaining six of the symptomatic children with SCD showed qualitative findings of AVN on conventional MRI (Fig. 2); these findings are summarized in Table 2.

The ADC values for the six symptomatic children who had AVN were compared with the other groups of children who did not have AVN. The mean and median ADC values in the hips with AVN were higher than the normal hips and SCD hips without AVN (Table 3). ADC values were significantly different among the subject groups (*P* < 0.001, Kruskal-Wallis test, Fig. 3) and in pairwise comparisons ADC values differed significantly between SCD children with AVN and the groups of normal children (*P* < 0.05), children with SCD who had hip symptoms but did not have

Table 2 Conventional MR imaging findings in symptomatic children with sickle cell disease

Patient ID	Findings	Hip avascular necrosis stage
1	Bone infarct in proximal diaphysis of the left femur	0
2	Bone infarct in left ischium	0
3	Small avulsion of left rectus femoris at the anterior inferior iliac spine	0
4	Infarcts in medial aspects of both iliac bones, lower lumbar spine and right pubic bone with intact acetabula and femoral heads	0
5	Infarcts in diaphyses, both femurs and iliac bones away from hip joints	0
6	Normal	0
7	Small focus of increased T ₂ - and decreased T ₁ -weighted signal intensity in the subchondral bone of the right femoral head	IA
8	Small focus of marrow edema in subchondral bone of the left femoral head and other regions of infarcts remote from the hips	IA
9	Subcondral fluid ~1/3 of left femoral head and edema in entire epiphysis and scattered bone infarcts remote from the hips	IC
10	Serpiginous bands of alternating low and high T ₂ -weighted signal intensity in 60–80% of the right femoral head	IIC
11	Small focus of bone marrow edema in the epiphysis with mild flattening of the femoral head	IVA
12	Bilateral disease with edema throughout majority of epiphyses intermixed with regions of low T ₁ and T ₂ signal intensity (sclerosis) and mild flattening of both femoral heads	IVA

Hip avascular necrosis is categorized using the University of Pennsylvania (Steinberg) staging system [10]

Table 3 Apparent diffusion coefficient values among normal and sickle cell disease children

	ADC value		
	Mean±SD	Median	95% confidence interval
Normal children	0.74±0.42	0.74	0.46–0.98
SCD without AVN	0.56±0.32	0.55	0.25–0.85
SCD with no detectable AVN in symptomatic femoral epiphysis	0.44±0.21	0.46	0.18–0.72
SCD with AVN (contralateral unaffected femoral epiphysis)	0.56±0.26	0.71	0.19–0.78
SCD with AVN (symptomatic femoral epiphysis)	1.60±0.34	1.57	0.86–2.10

ADC values are $\times 10^{-3} \text{ mm}^2/\text{s}$ calculated with $b=0$ and $b=500$ SCD sickle cell disease, AVN avascular necrosis, SD standard deviation

detectable AVN ($P<0.05$), and children with SCD who were asymptomatic for hip pathology and had no detectable hip AVN ($P<0.05$).

Further analysis was performed on the different patient groups to illustrate differences in ADC measurements due to the b-values used for the calculation. Table 4 depicts the relationship of ADC values among groups and the variation in ADC with selection of b-value, which may be due to signal rectification and/or tissue-specific decay of signal that is not mono-exponential with increasing b-value. Regardless of the b-values selected, the ADC was low in normal patients and the children without known or suspected AVN and elevated and less variable in children with AVN.

The variability of ADC values obtained within each subject was also measured by calculating the difference between ADC values in the left and right hips (dADC). The dADC was larger in the children with AVN who had unilateral disease than in the other groups (Table 5 and Fig. 4). Pairwise comparisons of the dADC showed that the dADC differed significantly between SCD children with

AVN and each of the three other subject groups without AVN (all $P<0.05$).

Discussion

This study demonstrates that DWI with ADC measurements may identify AVN in children with SCD. Detection of AVN is important not only to exclude other pathology [13] but also to alter therapy and to minimize irreversible damage to the growing skeleton [7]. In this study, elevated ADC values were found in the proximal femoral epiphyses affected by AVN. These hips affected by AVN had significant alterations in ADC values in comparison to normal children and SCD children with no MRI detectable hip joint pathology. These elevated ADC values in the affected hips are also similar in degree to those previously reported in children with Legg-Calvé-Perthes (LCP) disease: median ADC value = $1.32 \times 10^{-3} \text{ mm}^2/\text{s}$ in the proximal femoral epiphyses with LCP versus $0.54 \times 10^{-3} \text{ mm}^2/\text{s}$ in the contralateral control epiphyses [5].

Although imaging strategies already exist for detecting hip AVN including radiographs, conventional MRI and nuclear medicine [13], DWI with ADC measurements adds additional information. ADC measurements quantify altered water mobility. This feature of DWI is particularly attractive for quantifying AVN since the underlying pathophysiology in SCD is vaso-occlusion leading to ischemia and infarction.

Unlike the early detection of stroke where decreased ADC values indicate restricted diffusion from ischemia, most lesions in the musculoskeletal system, including the AVN detected in this study, have increased diffusion. Although epiphyseal ischemia may result in transient restriction of diffusion [3], most patients present days or weeks after the onset of symptoms, when the process is well established and diffusion has become elevated.

Furthermore, interpretation of an ADC value in the pediatric skeleton will likely have to take into account the age of the patient due to stages of tissue maturation in the femoral head epiphysis, e.g., infant cartilage and bone with hematopoietic marrow that transitions over time to adult-type

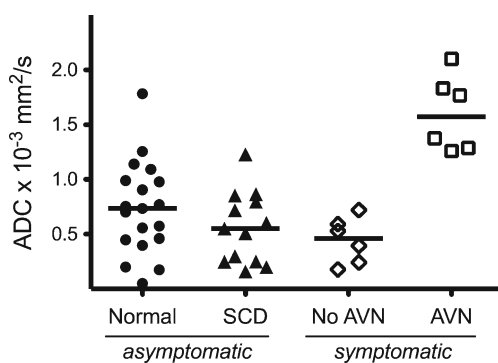


Fig. 3 Distribution of apparent diffusion coefficient (ADC) values in the study groups. ADC values are displayed only from right hip in normal subjects and in the group of children with sickle cell disease (SCD) who were both free of hip symptoms and had no detectable avascular necrosis (AVN). In SCD children with hip symptoms, ADC values are displayed from the symptomatic side. This symptomatic group is further subdivided into those with or without AVN as detected on conventional STIR, T₁- and T₂-weighted MRI. Bars depict median values

Table 4 Comparison of the apparent diffusion coefficient computed with various pairs of b-values

	$b=0$ & 250	$b=0$ & 500	$b=0$ & 750	$b=250$ & 500	$b=250$ & 750
Normal children	0.90±0.41	0.74±0.42	0.64±0.43	0.57±0.49	0.51±0.49
SCD without AVN	0.71±0.60	0.56±0.32	0.49±0.26	0.41±0.27	0.37±0.19
SCD with no detectable AVN in symptomatic femoral epiphysis	0.52±0.21	0.44±0.21	0.39±0.22	0.38±0.29	0.32±0.26
SCD with AVN (contralateral unaffected femoral epiphysis)	0.61±0.29	0.56±0.26	0.41±0.22	0.32±0.23	0.29±0.20
SCD with AVN (symptomatic femoral epiphysis)	1.82±0.32	1.60±0.34	1.55±0.33	1.33±0.57	1.36±0.43

ADC values are $\times 10^{-3}$ mm²/s calculated with the specified b-value pairs

SCD sickle cell disease, AVN avascular necrosis, SD standard deviation

trabecular bone with fatty marrow. However, we did not observe the expected lower ADC values or bimodal distribution of diffusion as previously reported for adult fatty bone marrow [14, 15]. Our higher ADC values in measurements in the normal children compared to adults may be due to a larger percentage of hematopoietic marrow in the children. Errors in signal rectification due to low signal intensity measurements on DWI may contribute a large amount of variability in the ADC measurements in normal marrow and marrow unaffected by AVN, particularly in the older subjects. Developing an age-based dataset of normal ADC values will be important, since the database may be used as a reference standard to identify and possibly quantify DWI abnormalities in pathological hips.

In addition to detecting AVN, this study reports ADC values in children with SCD without clinical symptoms or conventional imaging findings of AVN. The ADC values in this population who have a high likelihood of developing AVN were similar or slightly lower in value in comparison to normal children, but much lower than the high values in children with documented AVN. Although the marrow in SCD is hyperactive, this did not appear to have a substantial effect on ADC values since no statistically significant difference was detected between the normal and the SCD

Table 5 Absolute difference in apparent diffusion coefficient values between left and right hips

	dADC value		
	Mean±SD	Median	95% confidence interval
Normal children	0.15±0.10	0.13	0.08–0.23
Asymptomatic SCD without AVN	0.13±0.13	0.07	0.02–0.22
Symptomatic SCD without AVN	0.14±0.13	0.09	0.03–0.38
Symptomatic SCD with unilateral AVN	0.99±0.55	0.90	0.50–1.91

dADC values are $\times 10^{-3}$ mm²/s

SCD sickle cell disease, AVN avascular necrosis, SD standard deviation

groups without AVN. We propose that these low ADC values in children who have not yet developed AVN may serve as a baseline and future elevations in ADC would indicate pending ischemia and subsequent AVN. Thus, with further study of this technique, the ADC value may eventually prove to be a quantitative imaging biomarker of very early AVN in asymptomatic patients. Further studies in a larger cohort of SCD patients in various stages of disease will be needed to test this hypothesis. Beyond SCD, ADC measurements may also be applied to other groups of patients who are predisposed to AVN, e.g., bone marrow transplant, steroid therapy, marrow storage disorders and severe acute respiratory syndrome patients [16].

Future work will be necessary to establish whether an elevated ADC in children with SCD may herald the marrow/bone changes of vaso-occlusive disease before they manifest themselves as AVN by other detection strategies. We tested several combinations of b-value pairs and the data suggest that DWI with b-values selected at $b=0$ and 500 is a good starting point for future investigations in this area. Several limitations of this study include the small patient

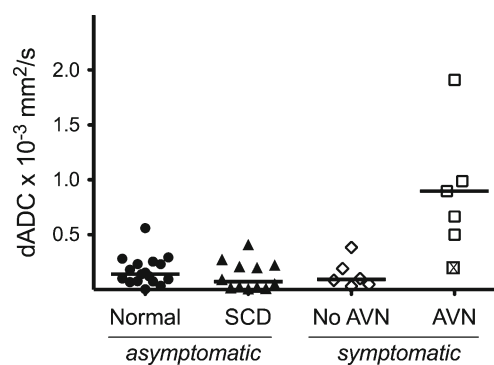


Fig. 4 Distribution of the difference in apparent diffusion coefficient (dADC) values between the left and right hips (absolute value) for each study group. The dADC illustrates the intrasubject variation in ADC measurements and depicts how the ADC is elevated in patients with unilateral avascular necrosis (AVN). The one patient with bilateral AVN is not used for calculation of the median for this group, is depicted with an “X” through the box and had only a small difference in left vs. right ADC values since both were elevated: $dADC=1.83-1.66=0.17 \times 10^{-3}$ mm²/s. Bars depict median values

population, the lack of follow-up for progression and new disease, the potential variability in normal ADC values in children based on the percentage of hematopoietic marrow and fatty marrow, and the potential for error when drawing free-hand ROI measurements. Further research is also necessary to determine whether ADC values reported here will serve either as a baseline of sickle cell marrow diffusion or as an indicator of very early onset of AVN.

In summary, this study demonstrates that ADC measurements may detect AVN in children with SCD. Alterations in ADC values may prove someday to be useful as an imaging biomarker of AVN in symptomatic patients with SCD. In addition, the ADC is low but variable in children with SCD who are asymptomatic and have no detectable AVN. This low ADC may serve as a baseline to monitor signs of future AVN.

Conclusion

This preliminary work suggests that an elevated apparent diffusion coefficient may be useful in helping support a diagnosis of avascular necrosis. However, marrow pathology such as the increased hematopoiesis in sickle cell disease may alter the apparent diffusion coefficient and must be taken into account when interpreting these measurements.

Acknowledgement The authors would like to thank Robert Mulkern and Jeffery Berman for insightful comments and analysis of ADC measurements obtained at varying field strengths.

References

- Mackenzie JD, Gonzalez L, Hernandez A et al (2007) Diffusion-weighted and diffusion tensor imaging for pediatric musculoskeletal disorders. *Pediatr Radiol* 37:781–788
- Menezes NM, Connolly SA, Shapiro F et al (2007) Early ischemia in growing piglet skeleton: MR diffusion and perfusion imaging. *Radiology* 242:129–136
- Jaramillo D, Connolly SA, Vajapeyam S et al (2003) Normal and ischemic epiphysis of the femur: diffusion MR imaging study in piglets. *Radiology* 227:825–832
- Li X, Qi J, Xia L et al (2008) Diffusion MRI in ischemic epiphysis of the femoral head: an experimental study. *J Magn Reson Imaging* 28:471–477
- Merlini L, Combescure C, De Rosa V et al (2010) Diffusion-weighted imaging findings in Perthes disease with dynamic gadolinium-enhanced subtracted (DGS) MR correlation: a preliminary study. *Pediatr Radiol* 40:318–325
- Yoo WJ, Kim YJ, Menezes NM et al (2011) Diffusion-weighted MRI reveals epiphyseal and metaphyseal abnormalities in Legg-Calvé-Perthes disease: a pilot study. *Clin Orthop Relat Res* 469:2881–2888
- Almeida A, Roberts I (2005) Bone involvement in sickle cell disease. *Br J Haematol* 129:482–490
- Milner PF, Kraus AP, Sebes JI et al (1991) Sickle cell disease as a cause of osteonecrosis of the femoral head. *N Engl J Med* 325:1476–1481
- Ramadan S, Mulkern RV (2010) Comment on ADC reductions in postcontrast breast tumors. *J Magn Reson Imaging* 31:262, author reply 263–264
- Steinberg ME, Steinberg DR (2004) Classification systems for osteonecrosis: an overview. *Orthop Clin North Am* 35:273–283
- Le Bihan D, Breton E, Lallemand D et al (1988) Separation of diffusion and perfusion in intravoxel incoherent motion MR imaging. *Radiology* 168:497–505
- Bland JM, Altman DG (1986) Statistical methods for assessing agreement between two methods of clinical measurement. *Lancet* 1:307–310
- Ejindu VC, Hine AL, Mashayekhi M et al (2007) Musculoskeletal manifestations of sickle cell disease. *Radiographics* 27:1005–1021
- Ababneh ZQ, Beloeil H, Berde CB et al (2009) In vivo lipid diffusion coefficient measurements in rat bone marrow. *Magn Reson Imaging* 27:859–864
- Mulkern RV, Schwartz RB (2003) In re: characterization of benign and metastatic vertebral compression fractures with quantitative diffusion MR imaging. *AJNR* 24:1489–1490, author reply 1490–1491
- Hong N, Du X, Nie Z et al (2005) Diffusion-weighted MR study of femoral head avascular necrosis in severe acute respiratory syndrome patients. *J Magn Reson Imaging* 22:661–664